NJC

Accepted Manuscript

Volume 1 | Number 1 | Jan 2013 | Pages 1–100

NJC

New Journal of Chemistry
www.rsc.org/njc

A journal for new directions in chemistry

ROYAL SOCIETY OF CHEMISTRY

cnrs

ROYAL SOCIETY OF CHEMISTRY

www.rsc.org/njc

Nano-zirconia as an excellent nano support for immobilization of sulfonic acid: A new, efficient and highly recyclable heterogeneous solid acid nanocatalyst for multicomponent reactions

Ali Amoozadeh∗, Salman Rahmani, Mehrnoosh Bitaraf, Fatemeh Bolghan Abadi and Elham Tabrizian

Faculty of Chemistry, Semnan University, Semnan 35131-19111, Iran

Abstract

Nano-zirconia-supported sulfonic acid [nano-ZrO_2-SO_3H (n-ZrSA)] is synthesized by immobilizing sulfonic acid groups on the surface of nano zirconium dioxide to produce novel heterogeneous reusable solid acid nanocatalyst. This new nanocatalyst is characterized by FT-IR spectroscopy, thermal gravimetric analysis (TGA), X-ray diffraction (XRD), field emission scanning electron microscopy (FE-SEM), transmission electron microscopy (TEM), Hammett acidity function and pH analysis. The introduced nano-zirconia-supported sulfonic acid is used as an efficient and recyclable catalyst for different heterocyclic multicomponent reactions such as synthesis of hexahydroquinoline, 1,8-dioxo-decahydroacridine, polyhydroquinoline and 1,8-dioxo-octahydroxanthene derivatives. Optimization of the reactions conditions was studied by central composite design (CCD) which is one of the most widely used response surface methodologies. The newly prepared heterogeneous solid acid nanocatalyst is easily separated and reused for five times without apparent loss of its catalytic activity that confirmed the stability of the covalent bonding of sulfonic acid groups. n-ZrSA has advantages such as low cost, low toxicity, ease of preparation, good stability, high reusability and operational simplicity.

Keywords: Nano-ZrO_2-supported sulfonic acid, Heterogeneous nanocatalyst, Multicomponent reaction, Design of experiment.

1. Introduction

∗ Corresponding author. Tel.: +98 (23) 33366177; fax: +98 (23) 33354110; e-mail: aamozadeh@semnan.ac.ir

Nowadays, using heterogeneous solid acid catalysts for chemical reactions and processes is widely expanded. Acid catalyzed organic synthesis is an important way to produce numerous organic products. Sulfuric, nitric, hydrochloric, phosphoric and fluorhydric acid are common homogeneous acid catalysts that are widely used in chemical synthesis and industrial processes.[1, 2] However, these catalysts are not environmentally benign because of their problems such as difficult separation from the products and corrosive properties. These disadvantages of homogeneous acid catalysts cause different problems such as using specialized reaction equipments, increasing operational difficulties, high consuming of energy and the formation of large amounts of waste products. In recent years, due to these drawbacks, the development of novel, low cost, nontoxic, well separable and recyclable heterogeneous catalysts has been the most important challenge of scientists.[3-8] Heterogenization of homogeneous catalysts by immobilization of sulfonic acid on various solid supports leads to the production of novel heterogeneous solid acid catalysts. This topic has attracted much attantion of extensive researcher during the past decade.[9-14] Transition metal nanoparticles are used as efficient catalysts for various synthetic organic transformations due to their high surface area-to-volume ratio and coordination sites which are mainly responsible for their catalytic activity.[15] These properties lead to their wide applications as excellent supports to produce new, efficient, nontoxic, environmental and reusable heterogeneous solid acid nanocatalysts.

Zirconium is one of the important transition metals on the earth crust (130 mg/kg), which is not found in nature as a native metal. The silicate mineral of zirconium, known as zircon ($ZrSiO_4$), is its principal source furthermore the zirconium dioxide (ZrO_2) is commercially available. It is mainly used as a refractory and opacifier, although it is used in small amounts as an alloying agent for its strong resistance to corrosion. Considering the multiple potential applications, zirconium dioxide is commonly used in numerous research

fields such as laboratory crucibles, metallurgical furnaces, as a refractory material,[16] oxygen sensors, fuel cell membranes, ceramics production,[17] protective coating on particles of titanium dioxide pigments,[17] strontium adsorption,[18] acylation of 1,n-diols [19] and other applications.

Given the excellent properties of ZrO_2 and the significance of heterogeneous solid acid catalysis, in continuation of our last studies about heterogeneous solid acid nanocatalysts,[20-22] we decided to investigate nano-ZrO_2 as a new nano support. As sulfonation with chlorosulfonic acid is a convenient, fast and efficient method for heterogenization of homogeneous catalysts after Zolfigol's report,[23] the catalytic properties of nano-ZrO_2 has been improved by its reaction with chlorosulfonic acid to produce nano-ZrO_2-supported sulfonic acid (nano-ZrO_2-SO_3H) (Scheme 1).
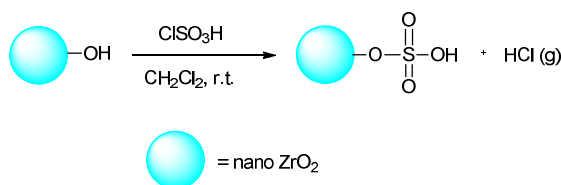
Scheme 1. Preparation of nano-ZrO_2-SO_3H (n-ZrSA).

2. Experimental

2.1. Materials and Instruments

Chemicals were purchased from Merck chemical companies. Thin-Layer Chromatography (TLC) on commercial plates of silica gel 60 F254 was used to monitor the progress of reactions. The products were characterized by FT-IR spectra, ^{1}HNMR, ^{13}CNMR and CHN analyzer. ^{1}H and ^{13}C NMR spectra which were recorded on Bruker Advance Spectrometer 400 & 500 MHz using $CDCl_3$-d and DMSO-d_6 as solvent. The chemical shifts are expressed in parts per million (ppm) and tetramethylsilane (TMS) was used as an internal reference. Elemental analyses were performed by Perkin Elmer CHN analyzer, 2400 series II. Melting points were recorded on a THERMO SCIENTIFIC 9100 apparatus. Wide angle X-ray

diffraction spectrum was obtained by a Siemens D5000 (Siemens AG, Munich, Germany) X-ray diffractometer using Cu-Ka radiation of wavelength 1.54 Å. Field emission scanning electron microscope (FE-SEM) images were carried out using Philips XL30 field emission scanning electron microscope (Royal Philips Electronics, Amsterdam, The Netherlands) instrument operating at 20 kV. The sample was mounted on a double sided adhesive carbon disk and sputter-coated with a thin layer of gold to prevent sample charging problems. Fourier transform infrared spectrum (FT-IR) was recorded on Shimadzo FT-IR 8400 instrument. The n-ZrSA sample was mixed with KBr powder and compressed into a pellet, wherein, the n-ZrSA powder was evenly dispersed. Thermo gravimetric analyses (TGA) were conducted on a Du Pont 2000 thermal analysis apparatus under air atmosphere at a heating rate of 5 °C/min.

2.2. Preparation of nano-ZrO$_2$

The zirconium dioxide nanoparticles were prepared through chemical precipitation method. 10 g ZrOCl$_2$.8H$_2$O was dissolved in 100 mL bidistilled water using hot plate magnetic stirrer. The desired volume of 2 M NaOH was added to the above mentioned precursor solution until the pH value became 10. After 15 minutes, the precipitate was filtered off, washed and dried at 120 °C overnight. The dried ZrO$_2$·nH$_2$O was calcined at different temperatures from 500 to 1200 °C at a rate of 10 °C/min and kept at the respective temperature for 1h.[24]

2.3. Preparation of nano-ZrO$_2$-SO$_3$H (n-ZrSA)

The chlorosulfonic acid (0.5 mL, 7.5 mmol) (CAUTION: a highly corrosive and water absorbant. Be careful when using this liquid. Protective gloves, protective clothing and eye and face protection equipment are also needed.) was added dropwisely over a period of 30 min under room temperature to the nano-ZrO$_2$ (3.08 g, 25 mmol) in dry CH$_2$Cl$_2$ (20 mL). A suction flask equipped with a constant-pressure dropping funnel and a gas inlet tube for conducting HCl gas over an adsorbing solution (i.e., water) was used. Stirring was continued until HCl evolution was finished. Then, the mixture was shaken for 30 min. A light cream

powder of nano-zirconia-supported sulfonic acid was obtained. Afterward, the CH_2Cl_2 was removed under reduced pressure and the solid powder was washed with ethanol (10 mL) and dried at 100 °C.

2.4. Investigating of n-ZrSA as a solid acid nanocatalyst for multicomponent one-pot synthesis of heterocyclic compounds

2.4.1. General procedure for the synthesis of hexahydroquinoline derivatives

In a typical experiment, 1,3-cyclic diketone (1 mmol), different aromatic aldehyde (1 mmol), ammonium acetate (1 mmol), malononitrile (1 mmol) and n-ZrSA (0.019 g) in solvent free condition were taken in a 25 mL round bottomed flask. The flask was stirred at 100 °C for an appropriate time. After completion of reaction (monitored by TLC), the reaction mixture was cooled, eluted with hot ethanol (5 mL), and centrifuged to collect the catalyst. The solvent was evaporated with reduced pressure to collect the formed precipitate. The crude product was recrystallized from ethanol to yield pure hexahydroquinoline derivatives.

2.4.2. General procedure for the synthesis of 1,8-dioxo-decahydroacridine derivatives

A mixture of 1,3-cyclic diketone (2 mmol), aromatic aldehyde (1 mmol), ammonium acetate (1 mmol) and n-ZrSA (0.027 g) in solvent free condition were taken in a 25 mL round bottomed flask. The flask was stirred at 100 °C for an appropriate time. The reaction mixture was cooled, eluted with hot ethanol (5 mL), and centrifuged to collect the catalyst. The solvent was evaporated with reduced pressure to collect the formed precipitate. The crude product was recrystallized from ethanol to yield pure 1,8-dioxo-decahydroacridines.

2.4.3. General procedure for the synthesis of polyhydroquinoline derivatives

In a 25 mL round bottomed flask, n-ZrSA (0.019 g) was added to the mixture of 1,3-cyclic diketone (1 mmol), aromatic aldehyde (1 mmol), ammonium acetate (1 mmol) and ethylacetoacetate (1 mmol) in solvent free conditions. The flask was stirred at 100 °C for an appropriate time. The reaction mixture was cooled, eluted with hot ethanol (5 mL), centrifuged to collect the catalyst. The solvent was evaporated with reduced pressure to

collect the formed precipitate. Recrystallization of crude product from ethanol yield pure polyhydroquinolines.

2.4.4. General procedure for the synthesis of 1,8-dioxo-octahydroxanthene derivatives

A well-stirred mixture of various 1,3-cyclic diketone (2 mmol), aromatic aldehyde (1 mmol) and n-ZrSA (0.039 g) as catalyst in a 25 mL round bottomed flask was heated at 100 °C (in an oil bath) in solvent free conditions for the appropriate time. Upon completion of the reaction (monitored by TLC), the reaction mixture was cooled, eluted with hot ethanol (5 mL), centrifuged to collect the catalyst and the solvent was evaporated with reduced pressure to give the crude product. The formed solid powder was washed with acetone. For further purification, it was crystallized from ethanol to afford pure 1,8-dioxo-octahydroxanthene derivatives.

2.4.5. General procedure for recycling of n-ZrSA

Recyclability of n-ZrSA (0.019 g) was examined for the synthesis of 2-amino-7,7-dimethyl-5-oxo-4-phenyl-1,4,5,6,7,8-hexahydroquinoline-3-carbonitrile between dimedone (1mmol), benzaldehyde (1 mmol), ammonium acetate (1 mmol) and malononitrile (1 mmol) under solvent free conditions for 15 minutes at 100 °C. After completion of the reaction, the nanocatalyst was separated from the production mixture by centrifuge, washed with ethanol (2 × 15 mL) and acetone (2 × 10 mL) to remove the organic compounds and dried in oven to be used in the next cycles. In every run, the yield of product was performed in constant time. This process was repeated six more times, affording the desired product in good yields, with undiminishing efficiency.

3. Results and Discussion

3.1. Characterization of nano-ZrO$_2$-SO$_3$H

Nano-zirconia-supported sulfonic acid was synthesized by immobilizing sulfonic acid groups on the surface of nano zirconium dioxide and characterized by FT-IR spectroscopy, thermal

gravimetric analysis (TGA), X-ray diffraction (XRD), field emission scanning electron microscopy (FE-SEM) and transmition electron microscopy (TEM), Hammett acidity function and pH analysis.

The FT-IR spectroscopy is employed to monitor the immobilization process by comparing the support and modified surface (Figure 1). In the graph **a** of Fig. 1, the absorbance bands at around 520, 580 and 727 cm^{-1} is due to Zr-O-Zr vibration, and the absorbance bands at around 3400-3500 cm^{-1} was certified to the adsorbed water (Fig. 1, graph **a** and **b**) which is consistent with the reported IR spectra for nano-ZrO$_2$.[25] In the graph **b** of Fig. 1, the absorption range in 1165-1248 and 1007-1065 cm^{-1} was certified the O=S=O asymmetric and symmetric stretching modes lies respectively. The S-O stretching mode lies in 560-608 cm^{-1}. These absorption and stretching obtained bands completely differ from stretching vibrations of O=S=O and S-O groups in sulfated zirconia.[26] According to the obtained results, presence of sulfonic acid group is proved which is consistent with the reported IR spectra of -SO$_3$H.[27]
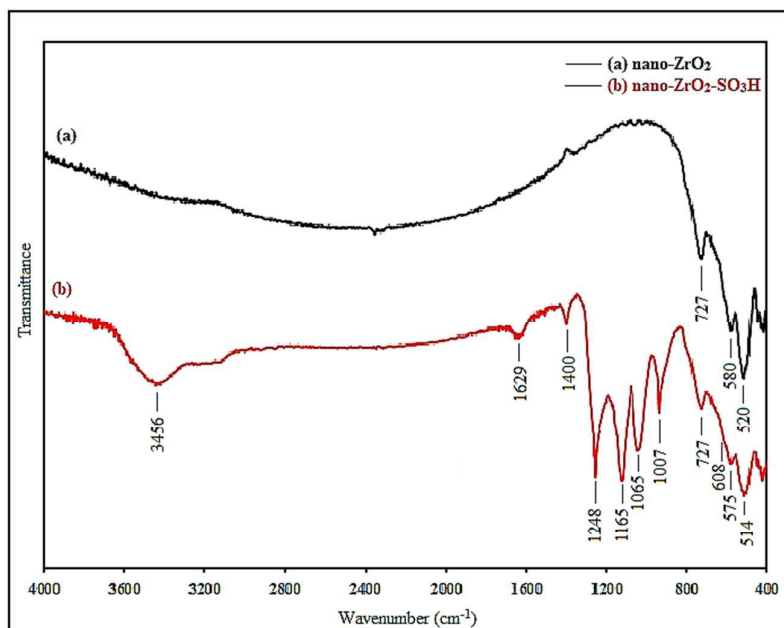
Fig. 1. The FT-IR spectra of (a) The nano-ZrO$_2$ powder and (b) nano-ZrO$_2$-SO$_3$H.

The thermal gravimetric analysis (TGA) was used to determine the percentage of the chemisorbed sulfonic acid group onto the surface of nano-ZrO$_2$. The TGA curve of nano-

ZrO_2 (Fig. 2a) displays a weight loss (5 wt.%) below 100 °C which corresponds to the loss of the physically adsorbed water. Likewise, there is a slight weight loss (4 wt.%) between 100 °C and 800 °C, which may contribute to the dehydroxylation of nano-ZrO_2.

In the TGA curve of nano-ZrO_2-SO_3H (Fig. 2b) three-stage decomposition is seen corresponding to different mass lose ranges. In the first region, a mass loss approximately 4% weight occurred below 100 °C that displayed that was attributable to the loss of trapped water from the catalyst. A mass loss of approximately 4% weight occurred between 100 and 330 °C that related to the slow mass loss of SO_3H groups. Finally, a mass loss of approximately 14% weight occurred between 330-700 °C that it was related to the sudden mass loss of SO_3H groups.[27, 28] From the TGA, it can be concluded that nano-ZrO_2-SO_3H could be safely used in organic reactions due to high thermal stability (up 150 °C).
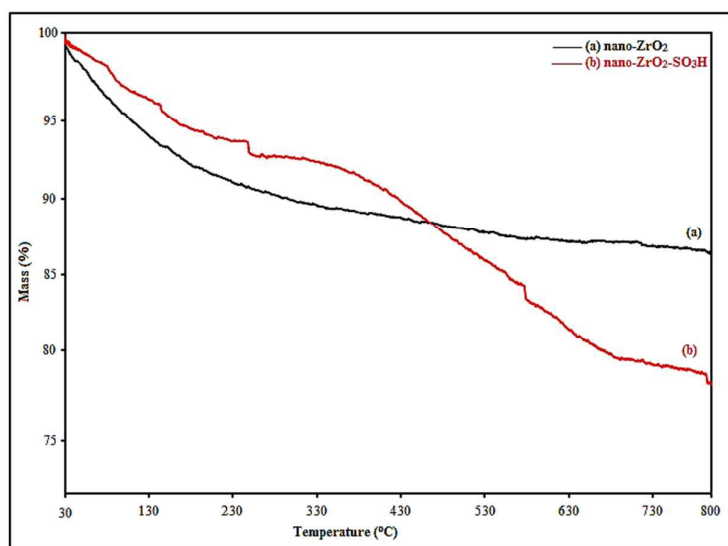
Fig. 2. TGA cure of (a) nano-ZrO_2 and (b) nano-ZrO_2-SO_3H.

The crystal phases of nano-ZrO_2 and n-ZrSA were examined by powder X-ray diffraction technique. The following peak signals with miler indices (100), (011), (110), (111), (111),(002), (200), (021), (211), (121), (112), (202), (022), (220), (122), (202), (013), (130), (310), (131), (131), (113), (213), (311), (023) and (222) in Fig. 3a confirm the formation of nano zirconium dioxide monoclinic crystal phase which coincides with JCPD 07-0343

standard. The average diameter of the nano-ZrO_2 powder was also determined from X-ray pattern using the Scherrer formula given as t=0.9λ/$B_{1/2}$cosθ, that t is the average crystal size, λ the X-ray wavelength used (1.54 Å), $B_{1/2}$ the angular line width at half maximum intensity and θ the Bragg′s angle. The average crystal size of the nano-ZrO_2 powder for 2θ = 27.875 º is calculated to be around 21.28 nm and average crystal size of the nano-ZrO_2-SO_3H powder for 2θ = 27.745 º is calculated to be around 21.27 nm. According to the PXRD data for the peak at 27.875 º (Fig. 3a), the maximum crystal growth of nano-ZrO_2 is 554. Fig. 3b illustrates XRD patterns of the modified nano-ZrO_2. As shown in Fig. 3b, the peak intensities of nano-ZrO_2-SO_3H (n-ZrSA) are almost the same as those of nano-ZrO_2 (Fig. 3a) indicating retention of the monoclinic crystal phase structure during functionalization of nano-ZrO_2.
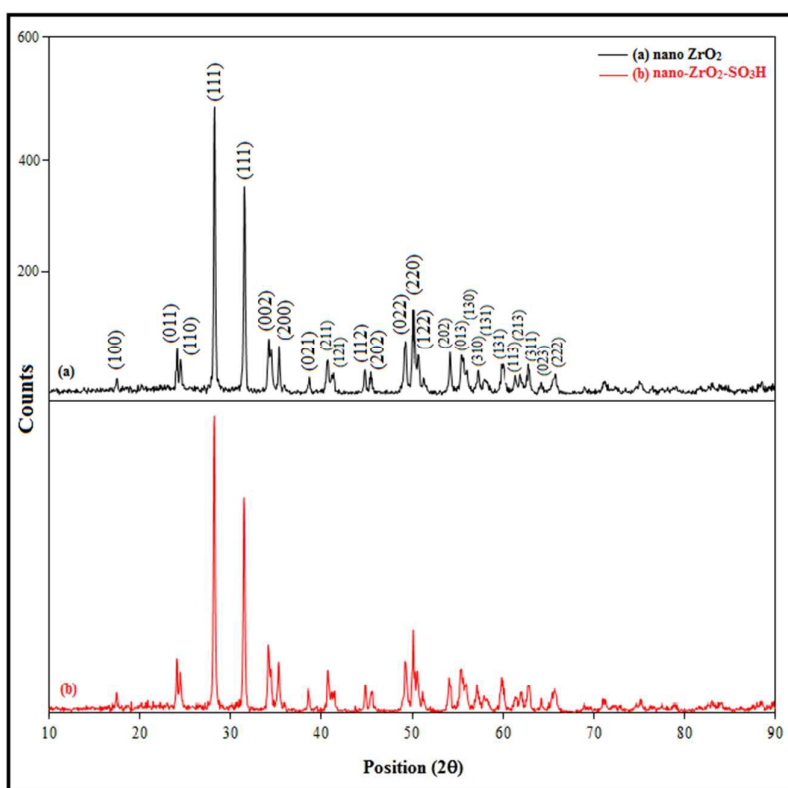
Fig. 3. The X-ray diffraction pattern of (a) the nano-ZrO_2 powder and (b) nano-ZrO_2-SO_3H.

The morphology of nano-ZrO_2 is shown in Fig. 4. The field emission scanning electron microscopy (FE-SEM) images of nano-ZrO_2 powder ascertain the spherical nano-ZrO_2 powder with a minimum particle sizes of about 30-40 nm (Fig. 4a, b). While the FE-SEM

images of n-ZrSA show nearly spherical nano particles with a minimum diameter of about

35-40 nm (Fig. 4c, d). It is clear that modification process has been achieved successfully.
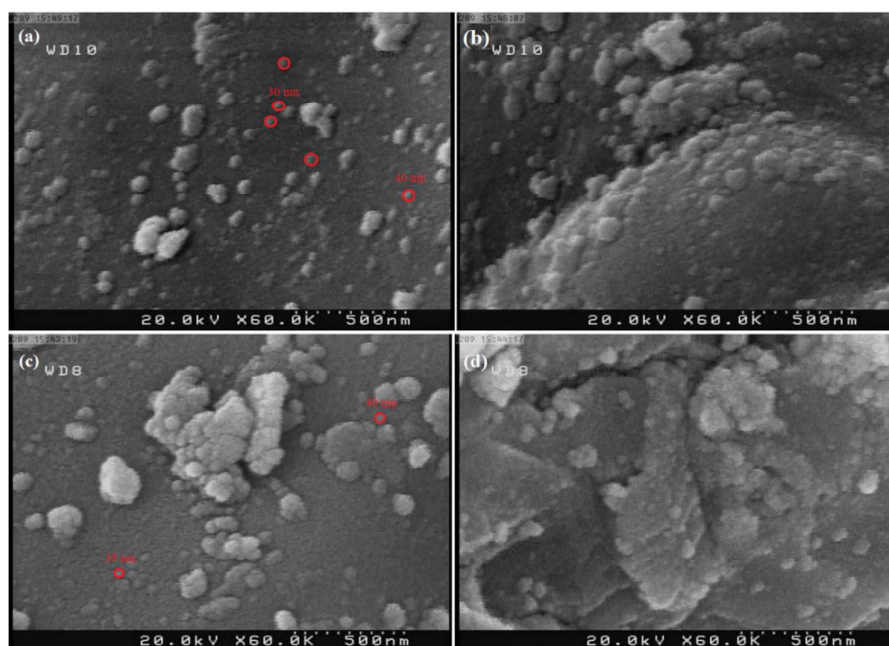
Fig. 4. The FE-SEM of (a,b) nano-ZrO_2 and (c,d) nano-ZrO_2-SO_3H.

Fig. 5 displays TEM images of nano-ZrO_2-SO_3H which confirms spherical-like and

nanometer-sized particles of the catalyst.
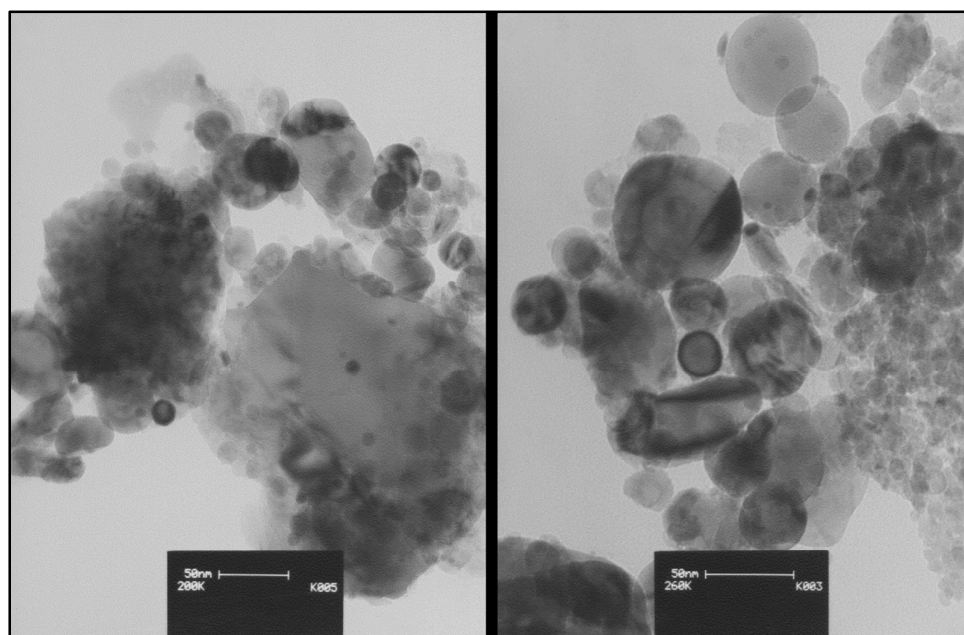
Fig. 5. The TEM images of nano-ZrO_2-SO_3H.

The acid strength of a catalyst can be effectively expressed by the Hammett indicator method [29] which can be calculated using the following equation:

$$H_0 = pK(I)_{aq} + \log([I]_s/[IH^+]_s),$$

Here, 'I' indicates the indicator base (mainly substituted nitroanilines) and $[IH^+]_s$ and $[I]_s$ are the molar concentrations of the protonated and unprotonated forms of the indicator, respectively. The pK(I)aq values are already known (for example the pK(I)aq value of 4-nitroaniline is 0.99) and can be obtained from many references. The value of $[I]_s/[IH^+]_s$ can be specified and calculated using the UV-visible spectrum cccording to the Lambert-Beer law. In this experiment, 4-nitroaniline was chosen as the basic indicator and CCl_4 as the solvent due to its aprotic property. The maximal absorbance of the unprotonated form of 4-nitroaniline was observed at 331.5 nm in CCl_4 as Fig. 6. Then, 20 mg of the catalyst was added to the solution and mixed for 30 min with magnetic stirring, and the UV spectrum of the solution was recorded. The absorbance of the unprotonated form of the indicator in n-ZrO_2-SO_3H decreased and was weak as compared to the sample of the indicator in CCl_4, which indicated that the acidic protons was trapped and the indicator was partially in the form of $[IH^+]$.
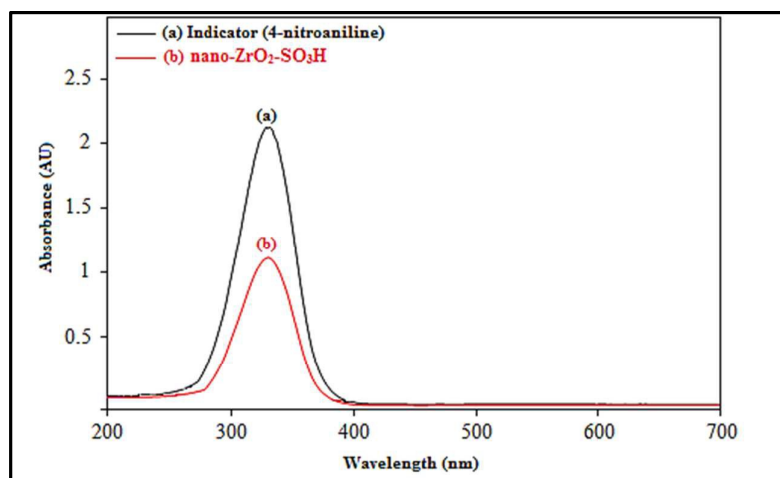
Fig. 6. Absorption spectra of (a) 4-nitroaniline (indicator) and (b) nano-ZrO_2-SO_3H (catalyst) in CCl_4.

The obtained results are listed in Table **1**, which shows the acidity strength of nano-ZrO_2-SO_3H. These results of the Hammett acidity function (H_0) also approve the synthesis of new catalyst with a good density of acid sites (-SO_3H groups) on the surface of nano-ZrO_2 (Table 1).

Table 1. Calculation of Hammett acidity function (H_0) of n-ZrSA.

Entry	Catalyst	A_{max}	$[I]_s$ (%)	$[IH^+]_s$ (%)	H_0
1	-	2.135	100	0	-
2	n-ZrSA	1.112	52.18	47.82	1.30

Condition for UV-visible spectrum measurement: solvent, CCl_4; indicator, 4-nitroaniline ($pK(I)_{aq}= 0.99$), $1.44*10^{-4}$ mol/L; catalyst, n-ZrSA (20 mg), 25 °C.

The acid capacities of n-ZrSA determined by acid-base potentiometric titration of the aqueous suspension of the weighed amount of thoroughly washed catalyst. For this purpose, the prepared n-ZrSA stored in vacuum desiccator over anhydrous silica gel, then, was dried in 120 °C for 6 hours. Next, the surface acidic protons of nano-ZrO_2-SO_3H were ion-exchanged with a saturated solution of NaCl (10 mL) by sonication. This process was repeated twice more, yielding 30 mL of proton-exchanged brine solution and the obtained solution was titrated by NaOH (0.01 M) solution in presence of pH meter. The loading of acid sites on the synthesized catalyst was obtained to about 3.9 mmol H^+/g of n-ZrSA.

The obtained results of characterization methods showed that sulfunic acid groups (-SO_3H) have been supported on the surface of nano-ZrO_2. It is notable that nano-ZrO_2-SO_3H acts as a Lewis and a Brønsted acid simultaneously in which nano-ZrO_2 functions as a Lewis acid and sulfonic acids function as the Brønsted. Brønsted acids could usually provide a hydrogen bond which can initiate the catalytic procedure. According to the obtained results, we expected better catalytic activity for nano-ZrO_2-supported sulfonic acid comparing with nano-ZrO_2. In order to approve this hypothesis, we have decided to investigate its catalytic activity in some of organic reactions.

3.2. Invastigating of nano-ZrO_2-SO_3H in one-pot multicomponent reactions

Considering our researches toward development of solid acid catalysts and evaluating their catalytic activity for the synthesis of organic compounds,[30-32] nano-titania-supported sulfonic acid[20] and nano-WO$_3$-supported sulfonic acid[21] as novel and efficient nanocatalysts were recently reported. On the basis of the informations obtained from the above mentioned studies, in this context, catalytic activity of nano-ZrO$_2$-supported sulfonic acid as a highly efficient, low cost, heterogeneous, reusable and inexpensive solid acid nanocatalyst was examined in multicomponent reactions for the synthesis of heterocyclic compounds such as hexahydroquinoline, 1,8-dioxo-decahydroacridine, polyhydroquinoline and 1,8-dioxo-octahydroxanthene derivatives. The structures of the some final products were well characterized by using spectral (IR, ^{1}H NMR, ^{13}C NMR) data.

3.2.1. Synthesis of hexahydroquinoline derivatives

Quinolines having a 1,4-dihydropyridine nucleus are very important compounds because of their pharmacological properties. These compounds have wide applications in medicinal chemistry, being used as antimalarial, anti-inflammatory, antiasthamatic, antibacterial antihypertensive, and tyrosine kinase inhibiting agents.[33-35] In recent years, several methods have been reported for the synthesis of hexahydroquinolines using of a variety of catalysts and reagents.[36-38]

However, many of these methods suffer from disadvantages such as long reaction times, unsatisfactory yields, harsh reaction conditions, expensive reagents, hazardous and toxic solvents or tedious work-up. Therefore, introduction of efficient and economical catalysts that solves these drawbacks is desirable. For this purpose, we decided to examine the applicability of n-ZrSA in the promotion of the synthesis of hexahydroquinolines. To study the role of catalyst, the reaction was carried out in catalyst free condition. The obtained result was not desirable (25%). So, the prepared nano-ZrO$_2$-SO$_3$H, was tested for the synthesis of hexahydroquinolines by multicomponent one-pot reaction between dimedone (**1**)

(1 mmol), benzaldehyde (**2**) (1 mmol), ammonium acetate (**3**) (1 mmol) and malononitrile (**4**)

(1 mmol) under solvent free condition as a model reaction (Scheme 2).
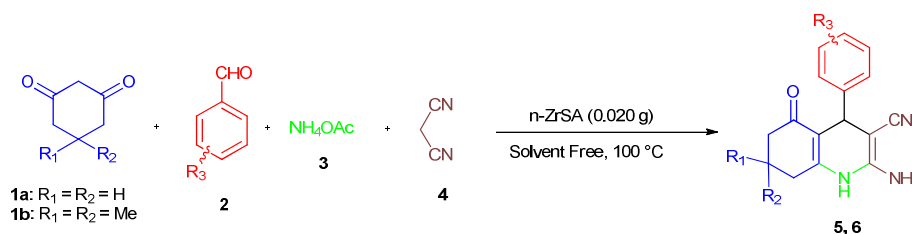
Scheme 2. Synthesis of hexahydroquinoline derivatives by nano-ZrO_2-SO_3H.

In order to find the optimal conditions for the synthesis of hexahydroquinoline

derivatives, the central composite design (CCD), one of the most applicable types of response

surface model (RSM), was applied. It has been accepted as a more effective optimization

method in attainment to improved responses via a fitted quadratic model which can be

expressed by following equation:

$$Y = \beta_0 + \sum_{i=1}^{4} \beta_i X_i + \sum_{i=1}^{4}\sum_{j=1}^{4} \beta_{ij} X_i X_j + \sum_{i=1}^{4} \beta_{ii} X_i{}^2$$

In which Y is response, Xi and Xj are independent variables, β_0 is the constant model,

β_i, β_{ii} and β_{ij} are coefficients for the linear, quadratic and interaction effects, respectively.

First of all, preliminary experiments were carried out to investigate the appropriate

parameters and to determine the experimental domain. Considering these experiments, the

effects of catalyst amount (X_1), temperature (X_2), and reaction time (X_3) were performed on

reaction yield as response. A five-level CCD of three independent variables with their

corresponding values is shown in Table S1 (in the supporting Information). Based on CCD

method, total number of experiments was found to be 20 which consisted of eight full

factorial points, six axial points and six central points. Conditions of 20 trials companied to

their respective yields are shown in Table S2 (in the supporting Information).

14

The analysis of variance (ANOVA) performed on the model can give valuable information on the significance of fitted model and its terms. From the ANOVA, as shown in Table 2, p-values of model and lack of fit are lower and higher than 0.05, respectively which means that, fitted model is significant at a confidence level of 95% and it does not require to reduce to lower orders. Also, the amounts of R-squared and adj R-squared are above 0.9 and close to each other which indicates fitted model has high accuracy and reliability in prediction of the reaction yield. In other words, there is a good agreement between experimental and the predicted responses which confirms the suitability of the following fitted model in terms of significantly linear, quadratic and interaction terms on the basis of their p-values.

$$Y = -544.56 + 21.00X_1 + 5.59X_2 + 14.23X_3 + 0.04X_1X_2 - 0.55X_1^2 - 0.03X_2^2 - 0.37X_3^2$$

Table 2. The results of ANOVA in CCD for the synthesis of 2-amino-7,7-dimethyl-5-oxo-4-phenyl-1,4,5,6,7,8-hexahydroquinoline-3-carbonitrile.

Source	Sum of Squares	df	Mean Square	F Value	p-value Prob > F
Model	4188.54	9	465.39	129.79	< 0.0001
X_1-Catalyst amount	713.91	1	713.91	199.09	< 0.0001
X_2-Temperature	43.42	1	43.42	12.11	0.0059
X_3-Time	1228.25	1	1228.25	342.53	< 0.0001
X_1X_2	18.24	1	18.24	5.09	0.0477
X_1X_3	8.86	1	8.86	2.47	0.1470
X_2X_3	0.097	1	0.097	0.027	0.8728
X_1^2	1134.36	1	1134.36	316.34	< 0.0001
X_2^2	135.38	1	135.38	37.75	0.0001
X_3^2	1224.22	1	1224.22	341.40	< 0.0001
Residual	35.86	10	3.59		
Lack of Fit	24.67	5	4.93	2.20	0.2030
Pure Error	11.19	5	2.24		
Cor Total	4224.40	19			
R^2= 0.99	Adj-R^2= 0.98	Pred-R^2= 0.95			

It can be realized from response equation that the X_1 has a more linear effect on the product yield, so the amount of catalyst can be considered as the main factor in progressing of the reaction.

In order to investigate the main interaction effects between two parameters on the yield of reaction, three-dimensional profiles of yield versus a pair of parameters were applied

(Fig. 7). According to their p-values, interaction of X_1X_2 is significant; it means that simultaneous increment of the catalyst amount and reaction temperature cause to increase the product yield until 0.020 g of the catalyst and 100 ºC of reaction temperature. While, higher loading of the catalyst and also the temperature, not only did not improve the yield to a higher extent, but also decreased the product yields most probably due to the formation of undesirable by-products.
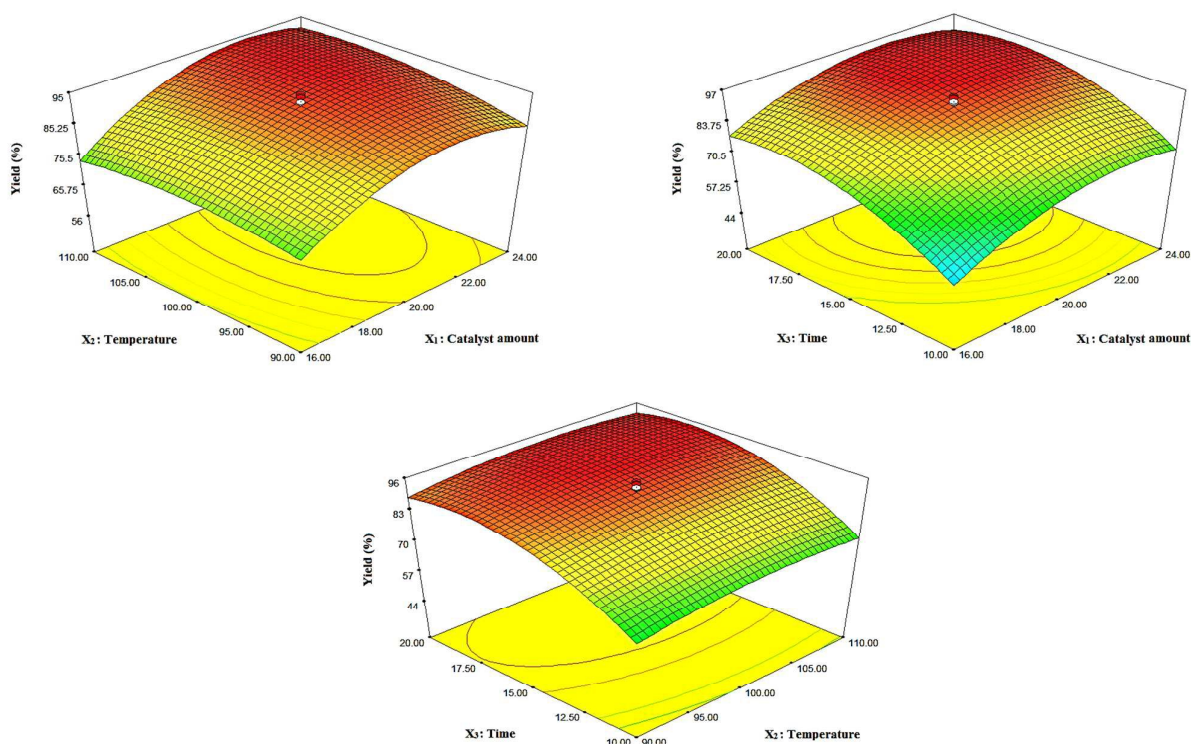
Fig. 7. Three dimensional response surfaces for the effect of factors on the reaction yield.

The main goal of this design was to optimize and maximize the yield of the reaction corresponded to the conditions of an experiment in which the response equation was maximized. In this work, determination of optimal conditions was done with the aid of desirability function by using Design-Expert 7.0.0. It was fistly selected desired goals for each factor and for response to obtain the maximum product yield with high desirability function (close to one). Then, conditions possessing high desirability were tested three times. Negligible difference between the average yields and the prediction values of software,

16

confirms the high accuracy and precision of optimum conditions.The results showed that 0.020 g of the catalyst, 100 ºC reaction temperatures, and 16 min reaction time were the optimum conditions for the synthesis of 2-amino-7,7-dimethyl-5-oxo-4-phenyl-1,4,5,6,7,8-hexahydroquinoline-3-carbonitrile.

To compare the efficiency of the solvent-free versus solvent conditions, the model reaction was performed under optimum condition. The results showed that higher yield and shorter reaction time were obtained when the reaction was carried out under solvent-free condition.

After optimizing the conditions, the generality of method was successfully studied by using various aromatic aldehydes (including aldehydes with electron-releasing substituents, electron-withdrawing substituents and halogens on the aromatic ring) and cyclic 1,3-diketone compounds. The obtained results are summarized in Table 3.

Table 3. Synthesis of hexahydroquinoline derivatives by nano-ZrO_2-SO_3H[a].

Entry	Ar	$R^1 = R^2$	Product	Time (min)	Yield[b] (%)	Melting point (ºC)	Literature m. p. (ºC)
1	-C_6H_5	H	**5a**	15	90	256-259	257 [36]
2	o-Cl-C_6H_4	H	**5b**	13	91	286-288	286 [36]
3	p-Cl-C_6H_4	H	**5c**	15	93	288-289	289 [36]
4	p-F-C_6H_4	H	**5d**	14	93	285-286	286 [36]
5	p-H_3C-C_6H_4	H	**5e**	23	89	258-260	258 [36]
6	p-H_3CO-C_6H_4	H	**5f**	25	87	275-278	278 [36]
7	m-O_2N-C_6H_4	H	**5g**	15	91	242-243	243 [36]
8	p-O_2N-C_6H_4	H	**5h**	13	93	259-262	260 [36]
9	-C_6H_5	CH_3	**6a**	16	94	234-237	275-277 [37]
10	p-H_3C-C_6H_4	CH_3	**6b**	22	91	>300	294-295 [37]
11	p-H_3CO-C_6H_4	CH_3	**6c**	22	90	287-290	289-293 [37]
12	m-O_2N-C_6H_4	CH_3	**6d**	14	93	280-284	282-283 [38]
13	o-Cl-C_6H_4	CH_3	**6e**	12	94	273-275	273-276 [37]
14	p-Cl-C_6H_4	CH_3	**6f**	14	95	288-291	290-291 [38]
15	p-F-C_6H_4	CH_3	**6g**	12	95	298-301	299-300 [38]
16	p-Br-C_6H_4	CH_3	**6h**	14	94	295-297	295-296 [38]
17	p-$(CH_3)_2$N-C_6H_4	CH_3	**6i**	25	90	>300	>300 [38]
18	2,6-Cl_2-C_6H_3	CH_3	**6j**	18	92	>300	>300 [38]

[a] Reaction conditions: **1** (1 mmol), **2** (1 mmol), **3** (1 mmol), **4** (1 mmol), n-ZrSA (0.020 g) under solvent-free condition at 100 °C.
[b] Isolated yield.

The present method not only affords the products in excellent yields but also avoids the problems associated with catalyst cost, handing, safety and pollution.

As indicated in Table 3, the reaction works easily for a vast variety of aromatic aldehydes with both electron-donating and electron-withdrawing groups and different cyclic di-ketones to give corresponding hexahydroquinoline derivatives in good to excellent yields. In almost all cases, the reactions proceeded smoothly within 12-25 minutes.

3.2.2. Synthesis of 1,8-dioxo-decahydroacridine derivatives

As acridines and their fused derivatives are important heterocycles that are known to possess multiple biological activities,[39] vasorelaxing,[40] anti-viral[41] and other applications, it was decided to develop the catalytic activity of nano-ZrO$_2$-SO$_3$H by investigating their synthesis. For this purpose, 1,8-dioxo-decahydroacridines was synthesized by condensation between dimedone (**1**) (2 mmol), benzaldehyde (**2**) (1 mmol) and ammonium acetate (**3**) (1 mmol) under solvent free conditions as a model reaction (Scheme 3).
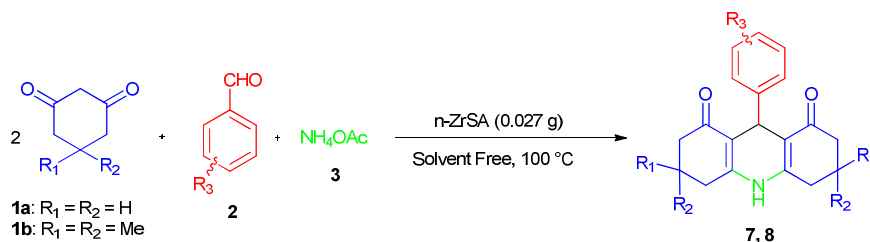
Scheme 3. Synthesis of 1, 8-dioxo-decahydroacridine derivatives by nano-ZrO$_2$-SO$_3$H.

Due to the effect of n-ZrSA, the synthesis of 1,8-dioxo-decahydroacridine was studied in catalyst free condition which the obtained result illustrate that the yield was low (8%). The activity of n-ZrSA is compared with the nano-ZrO$_2$. The obtained results showed that the n-ZrSA (91%, yield) was a more suitable option rather than the nano-ZrO$_2$ (6%, yield).

To examine the limitation and the scope of the reaction, the synthesis of different 1,8-dioxo-decahydroacridine derivatives have been investigated. The obtained results are summarized in Table 4.

New Journal of Chemistry Accepted Manuscript

Table 4. Synthesis of 1,8-dioxo-decahydroacridines by nano-ZrO$_2$-SO$_3$H.

Entry	Ar	R^1=R^2	Product	Time (min)	Yield^b (%)	Melting Point (°C)	Literature m. p. (ºC)
1	-C$_6$H$_5$	H	**7a**	50	89	280-282	279-280 [42]
2	p-Cl-C$_6$H$_4$	H	**7b**	45	92	295-297	297-298 [42]
3	p-Br-C$_6$H$_4$	H	**7c**	45	91	310-312	310-312 [42]
4	p-H$_3$C-C$_6$H$_4$	H	**7d**	55	87	254-256	255-257 [42]
5	p-HO-C$_6$H$_4$	H	**7e**	65	84	304-305	303-305 [42]
6	p-H$_3$CO-C$_6$H$_4$	H	**7f**	60	86	302-304	303-305 [42]
7	m-O$_2$N-C$_6$H$_4$	H	**7g**	45	93	280-282	282-284 [42]
8	-C$_6$H$_5$	CH$_3$	**8a**	45	91	290-291	290-291 [42]
9	p-H$_3$CO-C$_6$H$_4$	CH$_3$	**8b**	55	88	274-276	276-278 [42]
10	p-HO-C$_6$H$_4$	CH$_3$	**8c**	60	86	307-308	303-305 [42]
11	p-H$_3$C-C$_6$H$_4$	CH$_3$	**8d**	52	89	269-270	269-271 [43]
12	p-F-C$_6$H$_4$	CH$_3$	**8e**	40	93	292-294	292-294 [43]
13	p-Cl-C$_6$H$_4$	CH$_3$	**8f**	40	93	299-302	298-300 [42]
14	o-Cl-C$_6$H$_4$	CH$_3$	**8g**	38	92	221-224	220-222 [43]
15	p-Br-C$_6$H$_4$	CH$_3$	**8h**	40	92	308-311	313-315 [43]
16	p-O$_2$N-C$_6$H$_4$	CH$_3$	**8i**	35	94	312-314	290-292 [43]
17	m-O$_2$N-C$_6$H$_4$	CH$_3$	**8j**	37	93	282-284	293-295 [43]
18	2-Naphtaldehyde	CH$_3$	**8k**	50	88	358-359	265-267 [43]
19	p-(CH$_3$)$_2$N-C$_6$H$_4$	CH$_3$	**8l**	50	89	264-267	220-222 [43]

^{a} Reaction condition: **1** (1 mmol), **2** (1 mmol), **3** (1 mmol), n-ZrSA (0.027 g) in solvent free conditions at 100 °C.

^{b} Isolated yield.

As indicated in Table 4, the new conditions are very suitable for a vast variety of aromatic aldehydes with both electron-donating and electron-withdrawing groups to give corresponding 1,8-dioxo-decahydroacridine derivatives in good to excellent yields. In nearly all cases, the reactions proceeded smoothly within 35-65 minute. However, it is notable that substituted aromatic aldehydes with electron-withdrawing groups increase the rate of reaction (Table **4**, entries **2**, **3**, **7, 12-17**) probably by activating the carbonyl group as electrophile center. Contrarily in the case of electron-donating groups, the reaction was more slowly (Table **4**, entries **4-6** and **9-11**).

3.2.3. Synthesis of polyhydroquinoline derivatives

The synergistic use of solid acid catalyst and MCRs allows efficient synthesis of diverse N-containing heterocycles. Among these compounds, polyhydroquinoline and 1,4-dihydropyridines (1,4-DHPs) attracted immense attention because of their wide pharmaceutical activity range acting, for example, as vasodilator, bronchodilator,

New Journal of Chemistry Accepted Manuscript

antiatherosclerotic, antitumour, antidiabetic, geroprotective, and hepatoprotective agents, HIV protease inhibition and most importantly as calcium channel blockers.[44, 45]

Synthesis of polyhydroquinolines was performed by three component condensation between dimedone (**1**) (1 mmol), benzaldehyde (**2**) (1 mmol), ammonium acetate (**3**) (1 mmol) and ethylacetoacetate (**9**) (1 mmol) with 0.019 g of n-ZrSA at 100 °C under solvent free condition as a model reaction (Scheme 4).

1a: R$_1$ = R$_2$ = H
1b: R$_1$ = R$_2$ = Me
1c: R$_1$ = H, R$_2$ = Ph

n-ZrSA (0.019 g)
Solvent Free, 100 °C

10, 11, 12
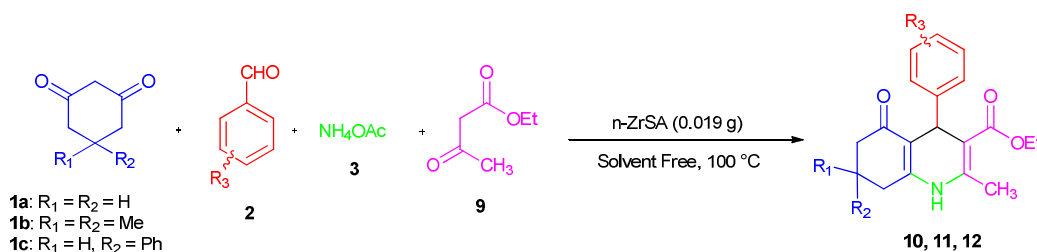
Scheme 4. Synthesis of polyhydroquinoline derivatives by nano-ZrO$_2$-SO$_3$H.

According to the low yield of the product reaction under catalyst free conditions (22%), the catalytic activity of n-ZrSA was compared with the nano-ZrO$_2$. The obtained results showed that the n-ZrSA (94%, yield) was a more suitable option rather than the nano-ZrO$_2$ (18%, yield). To examine the versatility of the optimum reaction conditions and its tolerance of functional groups on the hantzsch reaction, the synthesis of different polyhydroquinolines have been examined. The obtained results are summarized in Table 5.

Table 5. Synthesis of polyhydroquinolines by nano-ZrO$_2$-SO$_3$H[a].

Entry	Ar	R^1, R^2	Product	Time (min)	Yield[b] (%)	Melting Point (ºC)	Literature m. p. (ºC)
1	-C$_6$H$_5$	H	**10a**	37	91	239-241	240-242 [46]
2	p-H$_3$C-C$_6$H$_4$	H	**10b**	42	93	242-244	241-242 [47]
3	p-H$_3$CO-C$_6$H$_4$	H	**10c**	45	94	192-194	193-195 [47]
4	p-F-C$_6$H$_4$	H	**10d**	33	91	244-245	243-244 [47]
5	p-Cl-C$_6$H$_4$	H	**10e**	32	86	236-237	234-235 [47]
6	p-HO-C$_6$H$_4$	H	**10f**	50	84	220-221	220-222 [47]
7	o-O$_2$N-C$_6$H$_4$	H	**10g**	30	90	191-193	190-191 [47]
8	m-O$_2$N-C$_6$H$_4$	H	**10h**	32	89	199-201	198-200 [47]
9	p-O$_2$N-C$_6$H$_4$	H	**10i**	30	89	203-204	204-205[47]
10	-C$_6$H$_5$	CH$_3$	**11a**	35	94	210-211	202-204 [46]
11	o-O$_2$N-C$_6$H$_4$	CH$_3$	**11b**	30	96	203-205	207-208 [48]
12	m-O$_2$N-C$_6$H$_4$	CH$_3$	**11c**	32	94	170-171	182-184 [48]

13	p-O$_2$N-C$_6$H$_4$	CH$_3$	**11d**	28	96	207-209	202-203 [48]
14	o-Cl-C$_6$H$_4$	CH$_3$	**11e**	30	94	207-209	208-209 [46]
15	p-Cl-C$_6$H$_4$	CH$_3$	**11f**	30	95	243-245	245-247 [46]
16	p-F-C$_6$H$_4$	CH$_3$	**11g**	30	95	180-181	184-186 [48]
17	p-Br-C$_6$H$_4$	CH$_3$	**11h**	30	95	250-251	250-251 [48]
18	p-HO-C$_6$H$_4$	CH$_3$	**11i**	45	89	232-233	232-234 [46]
19	p-H$_3$CO-C$_6$H$_4$	CH$_3$	**11j**	45	90	255-256	258-259 [46]
20	p-H$_3$C-C$_6$H$_4$	CH$_3$	**11k**	40	91	283-284	260-262 [48]
21	p-(CH$_3$)$_2$N-C$_6$H$_4$	CH$_3$	**11l**	45	89	263-265	263-264 [46]
22	2,6-DiCl-C$_6$H$_3$	CH$_3$	**11m**	30	90	243-245	244-246 [46]
23	2-HO-5-Br-C$_6$H$_3$	CH$_3$	**11n**	50	88	246-248	247 [46]
25	-C$_6$H$_4$	H, Ph	**12a**	35	93	213-215	213-215 [46]
26	p-H$_3$CO-C$_6$H$_4$	H, Ph	**12b**	40	88	236-238	236-238 [46]
27	p-Cl-C$_6$H$_4$	H, Ph	**12c**	32	92	190-192	190-192 [46]

[a] Reaction condition: **1** (1 mmol), **2** (1 mmol), **3** (1 mmol), **9** (1 mmol), n-ZrSA (0.019 g) as catalyst under solvent-free conditions at 100 °C.
[b] Isolated yields.

As indicated in Table 5, the n-ZrSA catalyzed Hantzsch reaction very suitable for synthesis of a vast variety of polyhydroquinoline derivatives by condensation between different aromatic aldehydes with both electron-donating and electron-withdrawing groups and cyclic di-ketones to give corresponding product in good to excellent yields.

3.2.4. Synthesis of 1,8-dioxo-octahydroxanthene derivatives

Xanthenes, especially dioxo-octahydroxanthenes have developed as a powerful tool in organic synthesis due to their broad applications in different fields.[49-51] In recent years, several methods have been reported for the synthesis of octahydroxanthenes using of a variety of catalysts and reagents.[49, 52, 53]

The synthesis of 1,8-dioxo-octahydroxanthene derivatives was studied by condensation between dimedone (**1**) (2 mmol) and benzaldehyde (**2**) (1 mmol) under solvent free condition as a model reaction (Scheme 5). In order to explore the efficiency of n-ZrSA, the model reaction was carried out under the catalyst free conditions and compared with n-ZrSA and nano-ZrO$_2$. The obtained results showed higher yield for n-ZrSA (94%, yield) compared to catalyst free (21%, yield) and the nano-ZrO$_2$ (25%, yield).

1a: $R_1 = R_2 = H$
1b: $R_1 = R_2 = Me$
1c: $R_1 = H$, $R_2 = Ph$
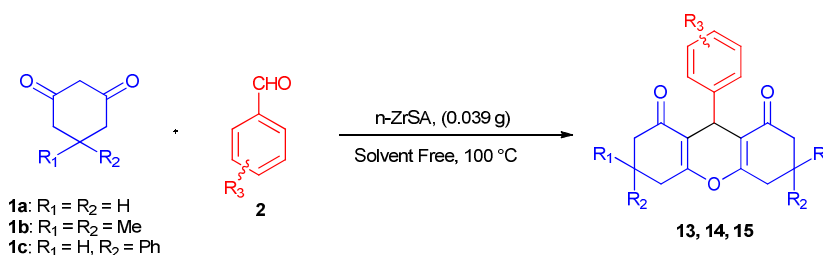
Scheme 5. Synthesis of 1,8-dioxo-octahydroxanthene derivatives by nano-ZrO_2-SO_3H.

The scope of octahydroxanthenes synthesis in presence of nano-ZrO_2-SO_3H was successfully studied by using various aromatic aldehydes (including aldehydes with electron-releasing substituents, electron-withdrawing substituents and halogens on the aromatic ring) and cyclic 1,3-diketone compounds. The results are summarized in Table 6.

Table 6. Synthesis of 1,8-dioxo-octahydroxanthene derivatives by nano-ZrO_2-SO_3H[a].

Entry	Ar	R^1	R^2	Product	Time (h)	Yield[b] (%)	Melting point (ºC)	Literature m. p. (ºC)
1	-C_6H_5	H	H	**13a**	2.1	92	213-215	213-215 [21]
2	p-H_3C-C_6H_4	H	H	**13b**	2.1	88	244-246	244-246 [21]
3	p-H_3CO-C_6H_4	H	H	**13c**	2.2	87	190-191	190-191 [21]
4	p-O_2N-C_6H_4	H	H	**13d**	1.8	93	234-236	234-236 [21]
5	p-Br-C_6H_4	H	H	**13e**	1.7	90	222-225	222-225 [21]
6	-C_6H_5	CH_3	CH_3	**14a**	2	94	203-204	205-206 [54]
7	o-H_3C-C_6H_4	CH_3	CH_3	**14b**	2.1	88	230-232	230-232 [21]
8	p-H_3C-C_6H_4	CH_3	CH_3	**14c**	2.2	89	212-214	220-222 [52]
9	p-H_3CO-C_6H_4	CH_3	CH_3	**14d**	2.2	90	242-244	250-251 [52]
10	p-HO-C_6H_4	CH_3	CH_3	**14e**	2.3	86	246-247	246-248 [55]
11	p-F-C_6H_4	CH_3	CH_3	**14f**	1.6	94	206-207	208-209 [55]
12	p-Cl-C_6H_4	CH_3	CH_3	**14g**	1.6	93	237-239	236-237 [52]
13	p-Br-C_6H_4	CH_3	CH_3	**14h**	1.7	90	264-267	263-265 [56]
14	o-O_2N-C_6H_4	CH_3	CH_3	**14i**	1.8	94	244-245	246-248 [55]
15	m-O_2N-C_6H_4	CH_3	CH_3	**14j**	1.8	92	168-169	167-168 [54]
16	p-O_2N-C_6H_4	CH_3	CH_3	**14k**	1.7	95	222-224	229-230 [52]
17	C_6H_5-CH=CH-	CH_3	CH_3	**14l**	2.3	84	256-258	256-258 [21]
18	2-Naphtaldehyde	CH_3	CH_3	**14m**	2.1	90	234-236	234-235 [21]
19	2-OH-5-Br-C_6H_3	CH_3	CH_3	**14n**	2.3	84	268-271	268-271 [21]
20	-C_6H_5	H	Ph	**15a**	2.1	90	196-198	196-198 [21]
21	p-Cl-C_6H_4	H	Ph	**15b**	2.2	89	234-236	234-236 [21]
22	p-H_3C-C_6H_4	H	Ph	**15c**	2.2	89	204-208	204-208 [21]
23	p-H_3CO-C_6H_4	H	Ph	**15d**	1.9	91	212-215	212-215 [21]

[a]Reaction conditions: cyclic-diketone (2 mmol), aromatic aldehyde (1 mmol), n-ZrSA (0.039 g) under solvent-free conditions at 100 °C.
[b]Isolated yield.

As showed in Table 6, fortunately the new catalyst also works very well for a vast variety of 1,8-dioxo-octahydroxanthene derivatives.

3.2.5. Reusability of the nano-ZrO_2-SO_3H

For practical applications of this new heterogeneous solid acid nanocatalyst, the level of reusability was also tested. The recycled catalyst could be reused for at least five times with no appreciable decrease in yield (Fig. 8). It signified that the nature of the catalyst remains intact after each run and SO_3H moiety was tightly anchored with nano-ZrO_2, probably through a covalent linkage.
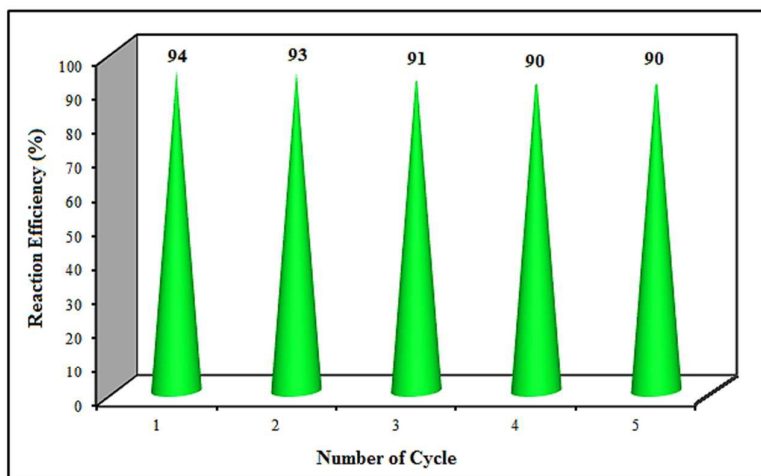
Fig. 8. Reusability of nano-ZrO_2-SO_3H

4. Conclusion

In summary, for the first time, the preparation and characterization of n-ZrO_2-SO_3H as an active and efficient heterogeneous acidic nanocatalyst was described. The catalytic activity of the catalyst was probed through the synthesis of hexahydroquinoline, 1,8-dioxo-octahydroacridine, polyhydroquinoline and 1,8-dioxo-octahydroxanthene derivatives by a one-pot multicomponent reactions strategy under solvent-free conditions. All the reactions work easily for a variety of aldehydes with both electron-donating and electron-withdrawing groups to give corresponding products in excellent yields. The catalyst was reused for five

consecutive cycles with consistent activity. Easy preparation and separation, high reusability

and excellent catalytic performance are the main superiorities of the synthesized catalyst.

Acknowledgements

References

1. M. D. González, Y. Cesteros, J. Llorca and P. Salagre, *J. Catal.*, 2012, **290**, 202-209.
2. J. A. Melero, R. van Grieken and G. Morales, *Chem. Rev.*, 2006, **106**, 3790-3812.
3. N. Ahmed and Z. N. Siddiqui, *J. Mol. Catal. A: Chem.*, 2014, **387**, 45-56.
4. R. D. Andrei, M. I. Popa, F. Fajula and V. Hulea, *J. Catal.*, 2015, **323**, 76-84.
5. M. Cao, D. Wu, W. Su and R. Cao, *J. Catal.*, 2015, **321**, 62-69.
6. S. Dabral, S. Nishimura and K. Ebitani, *Chem. Sus. Chem.*, 2014, **7**, 260-267.
7. R. Pagadala, S. Maddila, V. D. B. C. Dasireddy and S. B. Jonnalagadda, *Catal. Commun.*, 2014, **45**, 148-152.
8. S. Shabbir, Y. Lee and H. Rhee, *J. Catal.*, 2015, **322**, 104-108.
9. C.-H. Kuo, A. S. Poyraz, L. Jin, Y. Meng, L. Pahalagedara, S.-Y. Chen, D. A. Kriz, C. Guild, A. Gudz and S. L. Suib, *Green Chem.*, 2014, **16**, 785-791.
10. A. Mobaraki, B. Movassagh and B. Karimi, *Appl. Catal. A: General*, 2014, **472**, 123-133.
11. R. Parella and S. A. Babu, *Catal. Commun.*, 2012, **29**, 118-121.
12. Z. N. Siddiqui and N. Ahmed, *Appl. Organomet. Chem.*, 2013, **27**, 553-561.
13. H. Wan, Z. Wu, W. Chen, G. Guan, Y. Cai, C. Chen, Z. Li and X. Liu, *J. Mol. Catal. A: Chem.*, 2015, **398**, 127-132.
14. M. A. Zolfigol, A. Khazaei, M. Safaiee, M. Mokhlesi, R. Rostamian, M. Bagheri, M. Shiri and H. G. Kruger, *J. Mol. Catal. A: Chem.*, 2013, **370**, 80-86.
15. J. Deng, L.-P. Mo, F.-Y. Zhao, L.-L. Hou, L. Yang and Z.-H. Zhang, *Green Chem.*, 2011, **13**, 2576-2584.
16. Lide and R. David, *Journal*, 2007-2008, 42.
17. R. Nielsen, *Journal*, 2005.
18. H. Tel, A. Y., M. Eral, S. Sert, B. Cetinkaya and S. Inan, *Chem. Eng. J.*, 2010, **161**, 151-160.
19. V. Singh, V. Sapehiyia and G. L-Kad, *J. Mol. Catal. A: Chem.*, 2004, **210**, 119-124.
20. S. Rahmani, A. Amoozadeh and E. Kolvari, *Catal. Commun.*, 2014, **56**, 184-188.
21. A. Amoozadeh and S. Rahmani, *J. Mol. Catal. A: Chemical*, 2015, **306**, 96-107.
22. A. Amoozadeh, S. Golian and S. Rahmani, *RSC Advances*, 2015, **5**, 45974-45982.
23. M. A. Zolfigol, *Tetrahedron Lett.*, 2001, **57**, 9509-9511.
24. K. Geethalakshmi, T. Prabhakaran and J. Hemalatha, *Inter. Schol. Scien. Res. Innov.*, 2012, **6(4)**, 150-153.
25. M. Ranjbar, M. Yousei, M. Lahooti and A. Malekzadeh, *Int. J. Nanosci. Nanotechnol.*, 2012, **8**, 191-196.
26. G. D. Yadav, N. P. Ajgaonkar and A. Varma, *J. Catal.*, 2012, **292**, 99-110.
27. H. R. Shaterian, M. Ghashang and M. Feyzi, *Appl. Catal. A: Gen.*, 2008, **345**, 128-133.
28. M. A. Zolfigol, V. Khakyzadeh, A. R. Moosavi-Zare, G. Chehardoli, F. Derakhshan-Panah, A. Zare and O. Khaledian, *Scientia Iranica*, 2012, **19 (6)**, 1584-1590.
29. H. Xing, T. Wang, Z. Zhou and Y. Dai, *J. Mol. Catal. A: Chem.*, 2007, **264**, 53-59.
30. A. Amoozadeh, E. Tabrizian and S. Rahmani, *C. R. Chim.*, 2015, **18,** 848-857.
31. E. Tabrizian, A. Amoozadeh, S. Rahmani, E. Imanifar, S. Azhari, M. Malmir, *Chin. Chem. Lett.*, 2015, **26**, 1278-1282.
32. E. Kolvari, A. Amoozadeh, N. Koukabi, S. Otokesh and M. Isari, *Tetrahedron Lett.*, 2014, **55**, 3648-3651.

33. D. Doube, M. Bloun, C. Brideau, C. Chan, S. Desmarais, D. Eithier, J. P. Falgueyeret, R. W. Friesen, M. Girad, Y. Girad, J. Guay, P. Tagari and R. N. Yong, *Bioorg. Med. Chem. Lett.*, 1998, **8**, 1225-1230.
34. M. P. Maguire, K. R. Sheets, K. Mcvety, A. P. Spada and A. Ziberstein, *J. Med. Chem.*, 1994, **37**, 2129-2137.
35. G. Roma, M. D. Braccio, G. Grossi and M. Chia, *Eur. J. Med. Chem.*, 2000, **35**, 1021-1035.
36. A. R. Gholap, K. S. Toti, F. Shirazi, R. Kumari, M. K. Bhat, M. V. Deshpande and K. V. Srinivasan, *Bioorg. Med. Chem. Lett.*, 2007, **15**, 6705-6715.
37. S. Kumar, P. Sharma, K. K. Kapoor and M. S. Hunda, *Tetrahedron*, 2008, **64**, 536-542.
38. S. Tu, J. Zhang, X. Zhu, Y. Zhang, Q. Wang, J. Xu, B. Jiang, R. Jia, J. Zhang and F. Shi, *J. Heterocycl. Chem.*, 2006, **43**, 985-988.
39. J.-C. Xu, W.-M. Li, H. Zheng, Y.-F. Lai and P.-F. Zhang, *Tetrahedron*, 2011, **67**, 9582-9587.
40. O. Berkan, B. Sarac, R. Simsek, S. Yildirim, Y. Sarioglu and C. Safak, *Eur. J Med. Chem.*, 2002, **37(6)**, 519-523.
41. P. W. Groundwater and M. A. Munawar, *Adv. Heterocycl. Chem.*, 1997, **70**, 90-162.
42. K. S. Vahdat SM, Akbari M, Baghery S, *Arab. J. Chem.*, 2014.
43. M. M. Masoud Nasr-Esfahani, Tooba Abdizadeh, *C. R. Chim.*, 2015, **18**, 547–553.
44. A. Srivastava and C. Nizamuddin, *Indian. J. Heterocycl. Chem.*, 2004, **13(3)**, 261-264.
45. M. J. Wainwright, *Antimicrob. Chemother.*, 2011, **47(1)**, 1-13.
46. K. N. Otokesh S, Kolvari E, Amoozadeh A, Malmir M, Azhari S, *S. Afr. J.Chem.*, 2015, **68**, 15-20.
47. M. N. V. S. Shengkai Ko, Chunchi Lin and Ching-Fa Yao, *Tetrahedron Lett.*, 2005, **46**, 5771–5774.
48. R. B. Janardhan B, Crooks PA, *J. Saudi Chem. Soc.*, 2014, **5**, 722-726.
49. A. N. Dadhania, V. K. Raval and D. K. Raval, *J. Saudi Chem. Soc.*, 2014, **In Press**.
50. R. Giri, J. R. Goodell and C. Xing, *Bioorg. Med. Chem.*, 2010, **18**, 1456-1463.
51. N. Mulakayala, P. V. N. S. Murthy and D. Rambabu, *Bioorg. Med. Chem. Lett.*, 2012, **22**, 2186-2191.
52. S. Rostamizadeh, A. M. Amani, G. H. Mahdavinia, G. Amiri and H. Sepehrian, *Ultra. Sonochem.*, 2010, **17**, 306-309.
53. P. P. Salvi, A. M. Mandharea, A. S. Sartape, D. K. Pawar, S. H. Han and S. S. Kolekar, *C. R. Chim.*, 2011, **14**, 883-886.
54. P. S. Venkatesan K, Lahoti RJ, Srinivasan KV, *Ultr. Sonochem.*, **15**, 548-551.
55. Z. J. Jin TS, Wang AQ, Li TS, *Ultr. Sonochem.*, 2006, **13**, 220-223.
56. B. R. Kantevari S, Nagarapu L, *J. Mol. Catal. A. Chem.*, 2007, **269**, 53-60.

Graphical Abstract

Nano-zirconia-supported sulfonic acid as a novel, highly efficient and recyclable heterogeneous nanocatalyst is reported for the synthesis of multicomponent reactions